



1                                    **The role of a mid-air collision in drifting snow**

2    **Shuming Jia<sup>1,2</sup>, Zhengshi Wang<sup>1,2</sup>, Shumin Li<sup>1,2</sup>**

3    <sup>1</sup> State Key Laboratory of Aerodynamics, China Aerodynamic Research and Development

4    Center, Mianyang Sichuan 621000, China

5    <sup>2</sup> Computational Aerodynamics Institute, China Aerodynamics Research and Development

6    Center, Mianyang, Sichuan 621000, China

7    **Correspondence:** Zhengshi Wang ([wangzs@cardc.cn](mailto:wangzs@cardc.cn))



8    **Abstract.** Drifting snow, a common two-phase flow movement in high and cold areas,  
9    contributes greatly to the mass and energy balance of glacier and ice sheets and  
10   further affects the global climate system. Mid-air collisions occur frequently in  
11   high-concentration snow flows; however, this mechanism is rarely considered in  
12   current models of drifting snow. In this work, a three-dimensional model of drifting  
13   snow with consideration of inter-particle collisions is established; this model enables  
14   the investigation of the role of a mid-air collision mechanism in openly drifting snow.  
15   It is found that the particle collision frequency increases with the particle  
16   concentration and friction velocity, and the blown snow with a mid-air collision effect  
17   produces more realistic transport fluxes since inter-particle collision can enhance the  
18   particle activity under the same condition. However, the snow saltation mass flux  
19   basically shows a cubic dependency with friction velocity, which distinguishes it from  
20   the quadratic dependence of blown sand movement. Moreover, the snow saltation flux  
21   is found to be largely sensitive to the particle size distribution since the suspension  
22   snow may restrain the saltation movement. This research could improve our  
23   understanding of the role of the mid-air collision mechanism in natural drifting snow.



## 24 **1 Introduction**

25 As one of the most important indicators of global climate change, snow cover is  
26 widely distributed over high latitude regions (Mann et al., 2000; Gordon and Taylor,  
27 2009; Huang and Shi, 2017). Drifting snow is an important natural phenomenon in  
28 which air flow carries snow particles traveling near the surface, which not only  
29 profoundly changes the mass and energy balance of polar ice sheets (Déry and Yau,  
30 2002; Gallée et al., 2013; Huang et al., 2016) but also may induce various natural  
31 disasters, such as avalanches, landslides and mudslides (Christen et al.,  
32 2010; Schweizer et al., 2003; Sovilla et al., 2006). In-depth studies of the laws of snow  
33 particle motion and various influencing factors are essential for understanding this  
34 complex phenomenon.

35 Numerical simulations have become one of the most effective ways of exploring  
36 the blown snow movement, and plenty of drifting snow models have been established  
37 since the end of last century. Generally, drifting snow models can be divided into  
38 Euler-Euler models (Bintanja, 2000; Déry and Yau, 1999; Lehning et al.,  
39 2008; Schneiderbauer and Prokop, 2011; Uematsu et al., 1991; Vionnet et al.,  
40 2013; Xiao et al., 2000) and Euler-Lagrange models (Huang et al., 2016; Huang and  
41 Shi, 2017; Huang and Wang, 2015, 2016; Nemoto and Nishimura, 2004; Zhang and  
42 Huang, 2008; Zwaafink et al., 2014), in which snow particles are treated as one kind  
43 of continuous medium and individual particles, respectively. However, mid-air  
44 collisions, an important mechanism that influences the transportation of snow  
45 particles and the development of drifting snow, are hardly considered by current



46 models. The Lagrange tracking model can capture the inter-particle collision process  
47 more explicitly and directly, and thus is more suitable for establishing the mid-air  
48 collision model.

49 In this work, a trajectory-based mid-air collision model for drifting snow is  
50 established on the basics of a three-dimensional drifting snow model in the turbulent  
51 boundary layer, and the effects of mid-air collision on the snow transportation and  
52 particle motion are mainly explored. This paper is structured as follows: Sect. 2  
53 briefly introduces the model and method, Sect. 3 presents the model validation and  
54 simulation results, Sect. 4 discusses the results in detail, and Sect. 5 presents the  
55 conclusions.

## 56 **2 Model and method**

### 57 **2.1 Turbulent boundary layer**

58 The wind field is obtained from a large eddy simulation model of the Advanced  
59 Regional Prediction System (ARPS, version 5.3.3) (Xue et al., 2001). Considering the  
60 coupling effect between the snow particles and air flow, the fluid governing equations  
61 can be written as (Dupont et al., 2013; Vinkovic et al., 2006):

$$62 \quad \frac{\partial \rho}{\partial t} + \frac{\partial}{\partial x_i} (\rho \bar{u}_i) = 0 \quad (1)$$

$$63 \quad \frac{\partial \rho u_i}{\partial t} + \frac{\partial \rho u_i u_j}{\partial x_j} = -\frac{\partial \bar{p}^*}{\partial x_i} - \frac{\partial \tau_{ij}}{\partial x_j} + S_i \quad (2)$$

64 where  $\rho$  is the air density,  $t$  is time,  $x_i$  and  $u_i$  are the position coordinate and  
65 instantaneous wind velocity component, respectively, along three directions,



66  $p^* = p' - \alpha \nabla(\rho \mathbf{u})$  includes the pressure perturbation and damping term ( $\alpha$  is the  
 67 damping coefficient),  $\tau_{ij}$  is the sub-grid stress that is modeled by the Lagrangian  
 68 dynamic closure model of Meneveau et al. (1996), and  $S_i$  is the source term that  
 69 comes from the reaction force of the snow particles (Yamamoto et al., 2001):

$$70 \quad S_i = -\frac{1}{\rho V_{grid}} \sum_{s=1}^{N_p} F_D \quad (3)$$

71 where  $V_{grid}$  and  $N_p$  are the volume and the number of particles in the grid cell,  
 72 respectively.  $F_D = m_p V_r f(Re_p)/T_p$  is the fluid drag force, where  $m_p$  is the mass of  
 73 snow particle and  $V_r$  represents the relative speed between the snow particle and  
 74 wind field,  $T_p = \rho_p d_p^2 / 18 \rho \nu$  is the particle relaxation time, and  $\rho_p$  is the density of the  
 75 snow particle.  $Re_p = d_p V_r / \nu$  is the particle Reynolds number, where  $d_p$  is the particle  
 76 diameter and  $\nu$  is the kinematic viscosity of air.  $f(Re_p)$  can be expressed as (Clift  
 77 et al., 1978):

$$78 \quad f(Re_p) = \begin{cases} 1 & (Re_p < 1) \\ 1 + 0.15 Re_p^{0.687} & (Re_p \geq 1) \end{cases} \quad (4)$$

## 79 **2.2 Mid-air collision model**

80 The Lagrange particle tracking method is used to calculate the trajectory of each snow  
 81 particle. Considering the fluid drag force and gravity, the governing equation of  
 82 particle motion can be read as (Anderson and Haff, 1988; Lopes et al., 2013):

$$83 \quad \frac{dx_{pi}}{dt} = u_{pi} \quad (5)$$

$$84 \quad \frac{du_{pi}}{dt} = F_{di} + g_i \left(1 - \frac{\rho}{\rho_p}\right) \quad (6)$$



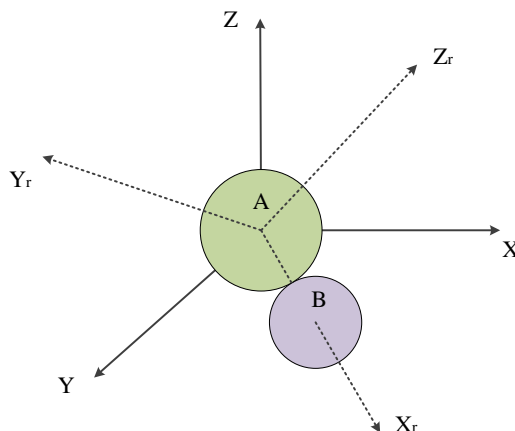
85 where  $x_p$  and  $u_p$  are the position and velocity of snow particle, respectively, and  $g$   
 86 is the gravitational acceleration.

87 During the process of particle motion, the judgment criterion for a mid-air  
 88 collision is  $l < (d_A + d_B)/2$ , in which  $l = \sqrt{\sum (x_{Ai} - x_{Bi})^2}$  is the center distance of  
 89 particle  $A$  and  $B$ . If particles  $A$  and  $B$  contact each other within a time step  $(t, t + \Delta t)$ ,  
 90 there must exist a root  $\delta t$  ( $0 < \delta t < \Delta t$ ) that satisfies the following relation:

$$91 \quad \frac{d_A + d_B}{2} = \sqrt{\sum ((x_{Ai} - u_{Ai}\delta t) - (x_{Bi} - u_{Bi}\delta t))^2} \quad (7)$$

92 in which the smaller root will be used if two roots exist. Thus, the collision time of  
 93 particles  $A$  and  $B$  is  $t + \delta t$ . To avoid repetition, there is the limitation condition of  
 94  $x_{A1} < x_{B1}$ .

95 To obtain particle information after the collision, the original coordinate system  
 96  $(X, Y, Z)$  is rotated to a new coordinate system  $(X_r, Y_r, Z_r)$ , as shown in Fig. 1, in  
 97 which the  $X_r$  axis points from the center of particle  $A$  to that of  $B$ . In this condition,  
 98 only the particle velocity component along the  $X_r$  axis is changed after the collision.



99  
 100 **Figure 1.** Schematic diagram of the rotation of the coordinate system.



101 Then, the particle velocity components ( $u_{Aci}$  and  $u_{Bci}$ ) in the new coordinate  
102 system can be calculated by the coordinate transformation algorithm. In addition, the  
103 particle velocity along the  $X_r$  axis after the collision in the new coordinate system  
104 can be expressed as:

$$105 \begin{cases} u'_{Acl} = u_{Acl} - \gamma d_B^3 (u_{Acl} - u_{Bcl}) \\ u'_{Bcl} = u_{Bcl} + \gamma d_A^3 (u_{Acl} - u_{Bcl}) \end{cases} \quad (8)$$

106 where  $\lambda = (1+e)/(d_A^3 + d_B^3)$  and  $e = 0.51v_n^{-1.4}$  is the recovery coefficient of ice  
107 (Supulver et al., 1995), in which  $v_n$  is the normal relative velocity of particle A and  
108 B.

109 Finally, the new coordinate system is rotated to the original location, and the  
110 particle velocity after the collision  $u'_{pi}$  can be obtained. The particle position after the  
111 collision can also be updated through  $x'_{pi} = x_{pi} - u_{pi} \delta t + u'_{pi} (\Delta t - \delta t)$ .

### 112 2.3 Simulation details

113 A computational domain of 2 m×1 m×1 m is adopted in this simulation. The grid  
114 number is 100×50×50, and grid stretch technology is used in the vertical direction  
115 (the finest grid scale is 2 mm). The turbulence inflow boundary is used (Lund et al.,  
116 1998), and the outlet is an open radiation boundary condition. The periodic boundary  
117 conditions are adopted along the spanwise direction. The inlet flow obeys the  
118 logarithmic wind profile with a boundary layer depth of 0.5 m and a roughness height  
119 of  $3.0 \times 10^{-5}$  m (Nemoto and Nishimura, 2004, 2001).

120 The aerodynamic entrainment scheme of (Zwaafink et al., 2014) is used to  
121 induce a drifting snow in the turbulent boundary layer. In addition, the splash function  
122 for snow (Sugiura and Maeno, 2000) is used to describe the grain-bed interaction.

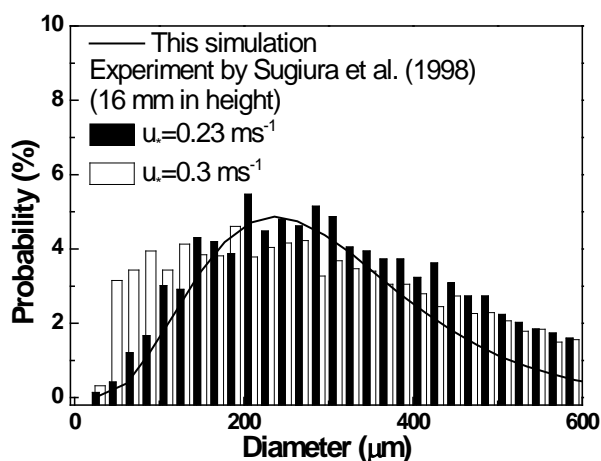


123 Furthermore, the fracturing of the snow particle is not considered during particle  
124 collision, and the rotation of the particle is also neglected because the duration time of  
125 inter-particle collision is very short.

### 126 3 Results

#### 127 3.1 Snow transport flux

128 The inter-particle collision within the drifting snow changes the trajectories of  
129 saltating particles, and further affect the structure and transport flux of the snow flow.  
130 Thus, the established drifting snow model is first verified by comparing the predicted  
131 snow transport flux with the measurements and other models.



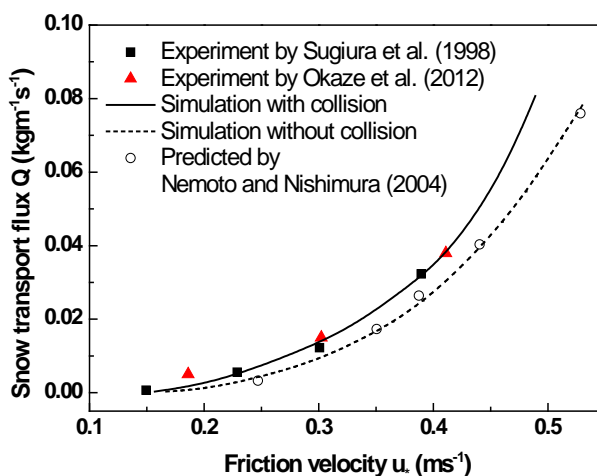
132  
133 **Figure 2.** Particle size distribution in the simulation.

134 The particle size distribution of the snow sample is similar to that adopted by  
135 Nemoto and Nishimura (2004), as shown in Fig. 2, which follows the gamma function  
136 with a mean diameter of 250  $\mu\text{m}$ . This distribution is also basically consistent with  
137 the experimental snow samples of Sugiura et al. (1998). Snow transport fluxes with  
138 and without a mid-air collision mechanism are shown in Fig. 3. From this figure, it





139 can be seen that without mid-air collisions, the snow transport flux at various friction  
140 velocities are consistent with the simulation results of Nemoto and Nishimura (2004),  
141 mainly because the same splash function is adopted.



142

143 **Figure 3.** Snow transport flux versus friction velocity.

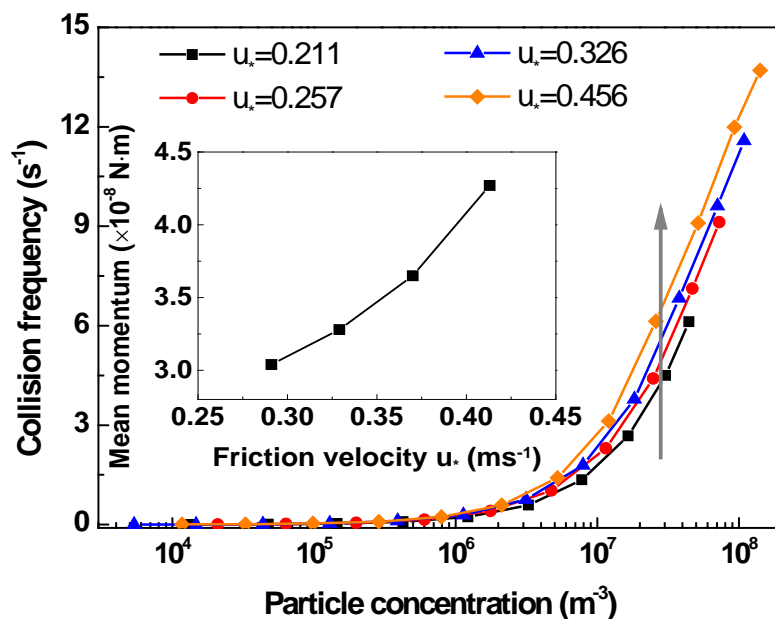
144 However, the snow transport flux is obviously enhanced with inter-particle  
145 collisions than without mid-air collisions, and the snow transport flux with mid-air  
146 collisions is obviously closer to the measurements (Okaze et al., 2012; Sugiura et al.,  
147 1998), which indicates that mid-air collisions are not negligible within drifting snow.  
148 At the same time, the enhanced proportion increases with increasing friction velocity.  
149 For example, at approximately the critical friction velocity, the snow transport flux  
150 with and without mid-air collisions is almost equal. However, when the friction  
151 velocity reaches  $0.489 \text{ ms}^{-1}$ , the enhanced proportion by mid-air collisions is up to  
152 38.97%. The reason could be that frequent collisions between higher and lower  
153 particles in the snow flow, on the one hand, increase the momentum of the impacting  
154 particles, and on the other hand, send the falling particles back to high altitude to



155 obtain more energy.

### 156 3.2 Collision frequency

157 The collision frequency under various friction velocities is shown in Fig. 4. It can be  
158 seen that the collision frequency is directly related to the particle concentration. When  
159 the particle concentration is below  $1.0 \times 10^6 \text{ m}^{-3}$ , inter-particle collisions rarely occur.  
160 However, with the further increment in the particle concentration, the frequency of the  
161 inter-particle collision event increases rapidly, and one particle may experience over  
162 10 collisions per second when the particle concentration is  $1.0 \times 10^8 \text{ m}^{-3}$ .



163

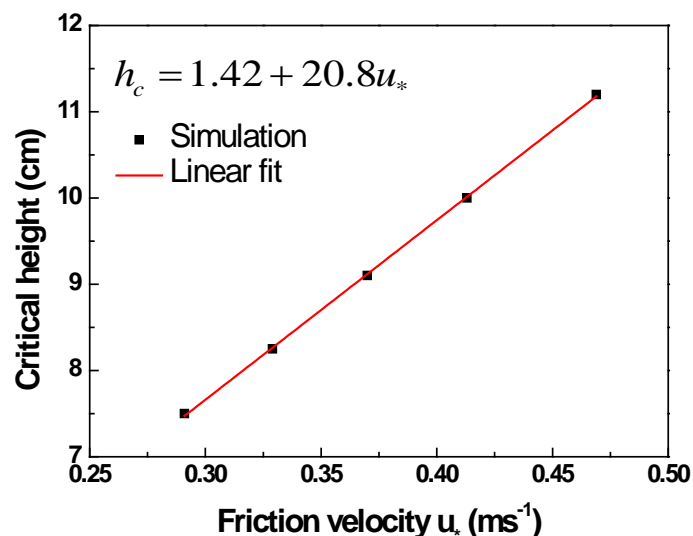
164 **Figure 4.** Inter-particle collision frequency versus particle concentration under  
165 various friction velocities (inset: mean particle momentum of saltating snow particle  
166 in drifting snow).

167 In addition, the collision frequency also increases with the friction velocity at the  
168 same particle concentration. The reason could be that particles are more active with



169 larger friction velocity, and as shown in the inset, the mean particle momentum tends  
170 to increase with friction velocity, which is also consistent with the experimental  
171 measurements (Nishimura et al., 2015; Nishimura and Hunt, 2000).

172 From the above analysis, drifting snow generally exists at a critical height, i.e.,  
173 mid-air collisions frequently occur below this height, while there are few collision  
174 events above this height. As shown in Fig. 5, the critical height  $h_c$  basically  
175 increases linearly with the friction velocity when the critical particle concentration of  
176  $1.0 \times 10^6 \text{ m}^{-3}$  is adopted, and the function of  $h_c = 1.42 + 20.8u_*$  properly describes the  
177 tendency.



178

179 **Figure 5.** Critical height for the mid-air collision in drifting snow.

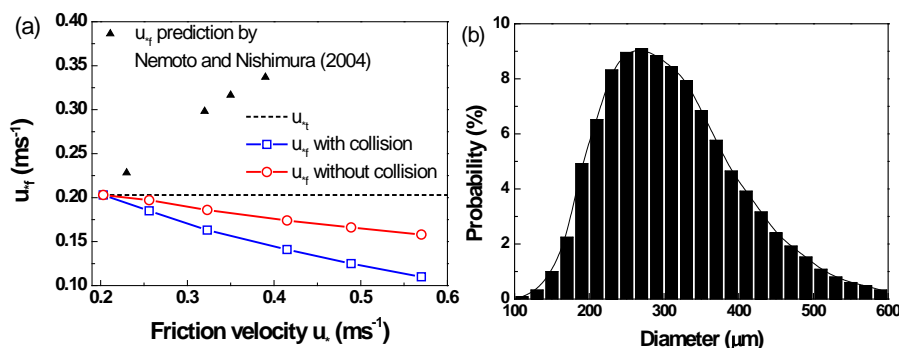
#### 180 **4 Discussions**

181 In steady-state drifting snow, part of the downward horizontal momentum flux in the  
182 saltation layer is carried by saltating snow particles, and thus the total downward  
183 momentum flux  $\tau$  equals the sum of the horizontal momentum fluxes due to particles



184  $\tau_p$  and the fluid  $\tau_f$ , that is,  $\tau = \tau_p + \tau_f$  (Kok et al., 2012; Raupach, 1991). The  
 185 residual fluid shear stress  $\tau_f$ , also called the impact threshold, represents the  
 186 threshold of the fluid shear stress that retains the particle splash process and is  
 187 commonly treated as a constant in the steady-state saltation (Bagnold, 1941; Owen,  
 188 1964).

189 However, several recent physically based numerical saltation models indicate  
 190 that  $\tau_f$  in fact decreases with the friction velocity mainly because the larger wind  
 191 speed higher in the saltation layer should be compensated by a decrease in the wind  
 192 speed lower in the saltation layer (Kok et al., 2012). This is also true for drifting snow,  
 193 as shown in Fig. 6(a). In this simulation, coarse snow particles are adopted since pure  
 194 saltation with least suspended snow is wanted, the particle size distribution is shown  
 195 in Fig. 6(b). It can be seen that the particle size is larger than 100  $\mu\text{m}$  because the  
 196 diameter of the suspension snow is basically smaller than 100  $\mu\text{m}$  (Gordon and Taylor,  
 197 2009; Huang and Wang, 2015; Nemoto and Nishimura, 2004; Nishimura and Hunt,  
 198 2000).



199  
 200 **Figure 6.** (a) Variation in the fluid stress versus friction velocity, and (b) particle size  
 201 distribution for the pure saltation simulation.



202            Additionally, the presence of mid-air collisions further decreases the impact  
203 threshold to a great extent. As shown in Fig. 6(a), under the same friction velocity  
204 condition, the residual fluid shear stress  $\tau_f$  with the mid-air collision effect is  
205 smaller than that without mid-air collisions, mainly because frequent inter-particle  
206 collisions can produce many high energy particles under the actions of momentum  
207 transfer among the particles and thus enhances saltation.

208            It is known that the saltation mass flux can be derived from the momentum  
209 balance in the saltation layer as (Kok et al., 2012; Sørensen, 2004):

$$210 \qquad Q = \rho(u_*^2 - u_{*f}^2)L / \Delta\bar{V} \qquad (9)$$

211 where  $u_{*f}$  is the critical impact friction velocity,  $L$  is the mean saltation length, and  
212  $\Delta\bar{V}$  is the mean velocity difference of the impact and lift-off particles. Many  
213 numerical and experimental investigations present the scaling of the saltation mass  
214 flux  $Q$  with  $u_*^3$  (Bagnold, 1941; Clifton et al., 2006; Nishimura and Hunt, 2000; Owen,  
215 1964; Vionnet et al., 2013) by assuming that the particle speeds can be linearly scaled  
216 with the friction velocity  $u_*$ , and  $u_{*f}$  is commonly approximate with the critical  
217 fluid friction velocity  $u_{*t}$ . Whereas the critical impact friction velocity  $u_{*f}$  may be  
218 larger or smaller than the critical fluid friction velocity  $u_{*t}$  as a matter of fact, as  
219 shown in Fig. 6(a).

220            For wind-blown sand movement, recent studies have proved that the saltation  
221 mass flux actually shows a quadratic dependency with the friction velocity since the  
222 mean particle speed in the saltation layer is independent of the friction velocity  
223 (Durán et al., 2011; Ho et al., 2011; Kok et al., 2012). For drifting snow, however, the



224 mean particle speed at the near surface is essentially proportional to the friction  
225 velocity (Nishimura and Hunt, 2000; Nishimura et al., 2015) probably due to the  
226 smaller response time of the snow particle, which supports the fact that the snow  
227 saltation flux typically shows a cubic dependency.

228 Interestingly, Nemoto and Nishimura (2004) reported an increasing tendency of  
229 the fluid stress  $\tau_f$  with the friction velocity when suspension snow is included, as  
230 shown in Fig. 6(a). This increase may be because suspended snow reduces the wind  
231 speed higher in the air, which in turn need a larger wind speed lower in the saltation  
232 layer to replenish the particle momentum. Thus, the suspension snow may restrain the  
233 saltation movement. The measurements of Nishimura and Hunt (2000) with various  
234 snow grain sizes also support this point.

235 In this way, the saltation mass flux (or residual fluid stress) of drifting snow  
236 largely depends on the particle size. For pure saltation movement as in above  
237 simulation (e.g., coarse grain size),  $\tau_f$  decreases with the friction velocity and  
238 results in a larger saltation flux. Whereas for drifting snow with considerable  
239 suspended snow particles,  $\tau_f$  may increase with friction velocity, and thus reduce  
240 the saltation mass flux. That is, snow samples with different grain sizes may have  
241 different saltation mass fluxes under the same wind condition. The particle borne  
242 stress  $\tau_p$  from the above simulation is approximately 4.5 times that predicted by the  
243 model of Nemoto and Nishimura (2004) when the friction velocity is  $0.39 \text{ ms}^{-1}$ , and  
244 thus, the snow saltation flux may be considerably different.

245 Most previous drifting snow models adopted by the mass balance studies of



246 glaciers of ice caps consider the saltation and suspension processes independently  
247 (Gallée et al., 2001; Lehning et al., 2008; Vionnet et al., 2013). From above analysis,  
248 this may increase the uncertainty of prediction with varying grain sizes. A coupling  
249 model that includes the interactions between saltation and suspension snows is  
250 necessary to model the drifting snow process more exactly.

## 251 **5 Conclusions**

252 In this work, a three-dimensional drifting snow model in the turbulent boundary layer  
253 with consideration of a mid-air collision mechanism is established based on tracking  
254 the trajectory of each snow particle; this model enables the exploration of the mid-air  
255 collision mechanism on the drifting snow process exactly.

256 In the traveling snow flow, mid-air collisions play an important role in enhancing  
257 the snow transport flux. In addition, there exists a critical particle concentration in  
258 which inter-particle collisions rarely occur below this value. However, above the  
259 critical concentration, the collision frequency as well as the role of inter-particle  
260 collisions is found to increase with the friction velocity.

261 Furthermore, mid-air collisions also enhances the particle activity, and thus  
262 further reduces the residual fluid stress during drifting snow conditions. The snow  
263 saltation flux is also found to be sensitive to particle size distribution of the snow  
264 samples because suspension snow may restrain saltation movement to a great extent,  
265 and the snow saltation flux may vary several times for different particle size  
266 distribution.

## 267 **Acknowledgements**



268 This work is supported by National key research and development program  
269 (2016YFC0500901), Forestry industry research special funds for key public welfare  
270 projects (201404306), National Natural Science Foundation of China (11772143) and  
271 111 Project, B14044.

## 272 **References**

273 Anderson, R. S., and Haff, P. K.: Simulation of Eolian Saltation, *Science*, 241,  
274 820-823, 1988.

275 Bagnold, R. A.: *The Physics of Wind Blown Sand and Desert Dunes*, Methuen,  
276 London, 1941.

277 Bintanja, R.: Snowdrift suspension and atmospheric turbulence. Part I: Theoretical  
278 background and model description, *Boundary-Layer Meteorology*, 95, 343-368, 2000.

279 Christen, M., Kowalski, J., and Bartelt, P.: RAMMS: Numerical simulation of dense  
280 snow avalanches in three-dimensional terrain, *Cold Regions Science & Technology*,  
281 63, 1-14, 2010.

282 Clift, R., Grace, J. R., and Weber, M. E.: *Bubbles, drops, and particles*, 263-264, 1978.

283 Clifton, A., Rüedi, J. D., and Lehning, M.: Snow saltation threshold measurements in  
284 a drifting-snow wind tunnel, *Journal of Glaciology*, 52, 585-596, 2006.

285 Déry, S. J., and Yau, M. K.: A Bulk Blowing Snow Model, *Boundary-Layer*  
286 *Meteorology*, 93, 237-251, 1999.

287 Déry, S. J., and Yau, M. K.: Large - scale mass balance effects of blowing snow and  
288 surface sublimation, *Journal of Geophysical Research Atmospheres*, 107, 8-17, 2002.

289 Dupont, S., Bergametti, G., Marticorena, B., and Simoëns, S.: Modeling saltation





290 intermittency, *Journal of Geophysical Research Atmospheres*, 118, 7109-7128, 2013.

291 Durán, O., Claudin, P., and Andreotti, B.: On aeolian transport: Grain-scale  
292 interactions, dynamical mechanisms and scaling laws, *Aeolian Research*, 3, 243-270,  
293 <https://doi.org/10.1016/j.aeolia.2011.07.006>, 2011.

294 Gallée, H., Guyomarc'H, G., and Brun, E.: Impact Of Snow Drift On The Antarctic  
295 Ice Sheet Surface Mass Balance: Possible Sensitivity To Snow-Surface Properties,  
296 *Boundary-Layer Meteorology*, 99, 1-19, 2001.

297 Gallée, H., Trouvilliez, A., Agosta, C., Genthon, C., Favier, V., and Naaim-Bouvet, F.:  
298 Transport of Snow by the Wind: A Comparison Between Observations in Adélie Land,  
299 Antarctica, and Simulations Made with the Regional Climate Model MAR,  
300 *Boundary-Layer Meteorology*, 146, 133-147, 2013.

301 Gordon, M., and Taylor, P. A.: Measurements of blowing snow, Part I: Particle shape,  
302 size distribution, velocity, and number flux at Churchill, Manitoba, Canada, *Cold  
303 Regions Science & Technology*, 55, 63-74, 2009.

304 Ho, T. D., Valance, A., Dupont, P., and Ould, E. M. A.: Scaling laws in aeolian sand  
305 transport, 2011, 1059-1062, 2011.

306 Huang, N., and Wang, Z. S.: A 3-D simulation of drifting snow in the turbulent  
307 boundary layer, *Cryosphere Discussions*, 9, 301-331, 2015.

308 Huang, N., Dai, X., and Zhang, J.: The impacts of moisture transport on drifting snow  
309 sublimation in the saltation layer, *Atmospheric Chemistry & Physics*, 16, 7523-7529,  
310 2016.

311 Huang, N., and Wang, Z. S.: The formation of snow streamers in the turbulent



- 312 atmosphere boundary layer, *Aeolian Research*, 23, 1-10, 2016.
- 313 Huang, N., and Shi, G.: The significance of vertical moisture diffusion on drifting  
314 Snow sublimation near snow surface, *Cryosphere*, 11, 3011-3021, 2017.
- 315 Kok, J. F., Parteli, E. J., Michaels, T. I., and Karam, D. B.: The physics of wind-blown  
316 sand and dust, *Reports on Progress in Physics Physical Society*, 75, 106901, 2012.
- 317 Lehning, M., Löwe, H., Ryser, M., and Raderschall, N.: Inhomogeneous precipitation  
318 distribution and snow transport in steep terrain, *Water Resources Research*, 44,  
319 278-284, 2008.
- 320 Lopes, A., M. G., Oliveira, L., A., Ferreira, Almerindo, D., Pinto, and J., P.: Numerical  
321 simulation of sand dune erosion, *Environmental Fluid Mechanics*, 13, 145-168, 2013.
- 322 Lund, T. S., Wu, X., and Squires, K. D.: Generation of Turbulent Inflow Data for  
323 Spatially-Developing Boundary Layer Simulations, *Journal of Computational Physics*,  
324 140, 233-258, 1998.
- 325 Mann, G. W., Anderson, P. S., and Mobbs, S. D.: Profile measurements of blowing  
326 snow at Halley, Antarctica, *Journal of Geophysical Research Atmospheres*, 105,  
327 24491-24508, 2000.
- 328 Meneveau, C., Lund, T. S., and Cabot, W. H.: A Lagrangian dynamic subgrid-scale  
329 model of turbulence, *Journal of Fluid Mechanics*, 319, 353-385, 1996.
- 330 Nemoto, M., and Nishimura, K.: Direct Measurement Of Shear Stress During Snow  
331 Saltation, *Boundary-Layer Meteorology*, 100, 149-170, 2001.
- 332 Nemoto, M., and Nishimura, K.: Numerical simulation of snow saltation and  
333 suspension in a turbulent boundary layer, *Journal of Geophysical Research*



- 334 Atmospheres, 109, D18206, 2004.
- 335 Nishimura, K., and Hunt, J. C. R.: Saltation and incipient suspension above a flat  
336 particle bed below a turbulent boundary layer, *Journal of Fluid Mechanics*, 417,  
337 77-102, 2000.
- 338 Nishimura, K., Yokoyama, C., Ito, Y., Nemoto, M., Naaim - Bouvet, F., Bellot, H.,  
339 and Fujita, K.: Snow particle speeds in drifting snow, *Journal of Geophysical*  
340 *Research Atmospheres*, 119, 9901-9913, 2015.
- 341 Okaze, T., Mochida, A., Tominaga, Y., Nemoto, M., Sato, T., Sasaki, Y., and Ichinohe,  
342 K.: Wind tunnel investigation of drifting snow development in a boundary layer,  
343 *Journal of Wind Engineering & Industrial Aerodynamics*, 104-106, 532-539, 2012.
- 344 Owen, P.: Saltation of uniform grains in air, *Plenum Press*, 41, 344-353, 1964.
- 345 Raupach, M. R.: Saltation layers, vegetation canopies and roughness lengths, *Springer*  
346 *Vienna*, 1, 83-96, 1991.
- 347 Sørensen, M.: On the rate of aeolian sand transport, *Geomorphology*, 59, 53-62,  
348 <https://doi.org/10.1016/j.geomorph.2003.09.005>, 2004.
- 349 Schneiderbauer, S., and Prokop, A.: The atmospheric snow-transport model:  
350 *SnowDrift3D*, *Journal of Glaciology*, 57, 526-542, 2011.
- 351 Schweizer, J., Jamieson, J. B., and Schneebeli, M.: Snow avalanche formation,  
352 *Reviews of Geophysics*, 41, 1-25, 2003.
- 353 Sovilla, B., Burlando, P., and Bartelt, P.: Field experiments and numerical modeling of  
354 mass entrainment in snow avalanches, *Journal of Geophysical Research*, 111, F03007,  
355 2006.



356 Sugiura, K., Nishimura, K., Maeno, N., and Kimura, T.: Measurements of snow mass  
357 flux and transport rate at different particle diameters in drifting snow, *Cold Regions*  
358 *Science & Technology*, 27, 83-89, 1998.

359 Sugiura, K., and Maeno, N.: Wind-Tunnel Measurements Of Restitution Coefficients  
360 And Ejection Number Of Snow Particles In Drifting Snow: Determination Of Splash  
361 Functions, *Boundary-Layer Meteorology*, 95, 123-143, 2000.

362 Supulver, K. D., Bridges, F. G., and Lin, D. N. C.: The Coefficient of Restitution of  
363 Ice Particles in Glancing Collisions: Experimental Results for Unfrosted Surfaces,  
364 *Icarus*, 113, 188-199, 1995.

365 Uematsu, T., Nakata, T., Takeuchi, K., Arisawa, Y., and Kaneda, Y.:  
366 Three-dimensional numerical simulation of snowdrift, *Cold Reg.sci.technol*, 20,  
367 65-73, 1991.

368 Vinkovic, I., Aguirre, C., Ayrault, M., and Simoëns, S.: Large-eddy Simulation of the  
369 Dispersion of Solid Particles in a Turbulent Boundary Layer, *Boundary-Layer*  
370 *Meteorology*, 121, 283, 2006.

371 Vionnet, V., Martin, E., Masson, V., Guyomarc'H, G., Naaimbouvet, F., Prokop, A.,  
372 Durand, Y., and Lac, C.: Simulation of wind-induced snow transport in alpine terrain  
373 using a fully coupled snowpack/atmosphere model, *Cryosphere Discussions*, 7,  
374 2191-2245, 2013.

375 Xiao, J., Bintanja, R., Déry, S. J., Mann, G. W., and Taylor, P. A.: An Intercomparison  
376 Among Four Models Of Blowing Snow, *Boundary-Layer Meteorology*, 97, 109-135,  
377 2000.



378 Xue, M., Droegemeier, K. K., Wong, V., Shapiro, A., Brewster, K., Carr, F., Weber, D.,  
379 Liu, Y., and Wang, D.: The Advanced Regional Prediction System (ARPS) – A  
380 multi-scale nonhydrostatic atmospheric simulation and prediction tool. Part II: Model  
381 physics and applications, *Meteorology & Atmospheric Physics*, 76, 143-165, 2001.  
382 Yamamoto, Y., Potthoff, M., Tanaka, T., Kajishima, T., and Tsuji, Y.: Large-eddy  
383 simulation of turbulent gas-particle flow in a vertical channel: effect of considering  
384 inter-particle collisions, *Journal of Fluid Mechanics*, 442, 303-334, 2001.  
385 Zhang, J., and Huang, N.: Simulation of Snow Drift and the Effects of Snow Particles  
386 on Wind, *Modelling & Simulation in Engineering*, 2008, 2008.  
387 Zwaaftink, C. D. G., Diebold, M., Horender, S., Overney, J., Lieberherr, G., Parlange,  
388 M. B., and Lehning, M.: Modelling Small-Scale Drifting Snow with a Lagrangian  
389 Stochastic Model Based on Large-Eddy Simulations, *Boundary-Layer Meteorology*,  
390 153, 117-139, 2014.